Stereochemical composition–properties relationships in isotactic polypropylenes obtained with different catalyst systems

Ezio Martuscelli† and Maurizio Avella
Istituto di Ricerca su Tecnologia dei Polimeri e Reologia del CNR, via Toiano 6, Arco Felice (NA), Italy

and Anna Laura Segre and Enrico Rossi
Istituto di Strutturistica Chimica 'G. Giacomello' CNR Monterotondo Stazione, Roma

and Giovanni Di Drusco*, Paolo Galli and Tonino Simonazzi*****
**Himont Inc, USA*
***Montepolimeri, Milano, Italy*
****Himont Centro Ricerche Giulio Natta Ferrara, Italy*
(Received 10 February 1984)

The influence of stereochemical composition of the radial growth rate of spherulites, the nucleation density, the overall rate of crystallization and the thermal behaviour of fractions of iPP samples synthesized with different catalyst systems (low, high and very high yield) was investigated. The study used ^{13}C n.m.r., differential scanning calorimetry (d.s.c.) and optical microscopy. The ^{13}C n.m.r. analysis showed that due to the presence of catalytic sites with different stereoregulating capability the catalyst system produces polypropylene with different stereoregularity. It was found that the growth rate of spherulites and the overall rate of crystallization are strictly related to the stereochemical structure of the polypropylene. Moreover, for the low yield iPP, phenomena of secondary crystallization were observed by Avrami analysis of the overall kinetics. Values of the equilibrium melting temperature (T_m), energy of nucleation ($\Delta\phi^*$) and surface free energy of folding (σe) of iPP lamellar crystals have been determined according to the kinetic theory of polymer crystallization. The values of such thermodynamic quantities as well as the thermal behaviour of various iPP are strongly dependent upon the amount and distribution of configurational irregularities existing along the chains and upon the molecular mass distribution.

(Keywords: catalysts; isotacticity; polypropylene; crystallization; melting; stereochemical composition)

INTRODUCTION

In previous works we have studied the influence of stereochemical composition on the crystallization, thermal behaviour and the morphology of fractions of isotactic polypropylene (iPP) crystallized both from dilute solution and from the melt[1,2].

Samples of iPP were prepared in the laboratory using a traditional Ziegler–Natta catalyst system (δ-$TiCl_3$ and $Al(C_2H_5)Cl$ in toluene at 76°C or VCl_3 and $Al(C_2H_5)_3$ at 15°C). Fractions with different degrees of stereoregularity were obtained by extractions with suitable solvents and/or by isothermal fractional crystallization. The stereochemical pentad population was determined by ^{13}C n.m.r. analysis. It was found that in the case of iPP fraction obtained by using Ti based catalysts both the equilibrium dissolution and melting temperatures (T_d and T_m, respectively) decrease with decrease in the percentage of isotactic pentad. For samples of iPP completely free of configurational defects a value of 181°C was extrapolated for the equilibrium melting temperature (171°C for the equilibrium dissolution temperature)[1]. An almost invariance of T_d and T_m with the isotactic pentad content was observed in the case of fractions of iPP obtained by using vanadium based catalysts. These results indicated that the thermal and dissolution behaviour of the iPP fraction is determined not only by the stereochemical composition but also by other variables which depend on the catalyst system adopted.

As far as the overall rate of crystallization is concerned, it was found that at constant T_c, this quantity decreased with increases in the stereochemical defects whereas at a given ΔT the converse occurs. In the case of more defective iPP fractions, distinct phenomena of secondary crystallization were observed[2].

In the present paper, we report the results of an investigation of the influence of stereochemical composition on the radial growth rate of spherulites, the nucleation density, the overall rate of crystallization and the thermal behaviour of fractions of iPP obtained in industrial pilot plants by using three different catalytic systems. These catalysts, developed by Montepolimeri[3], are termed Low-Yield (LY), High-Yield (HY) and Very-High-Yield (VHY), depending on their activity. The LY system is basically a traditional $TiCl_3$-based Ziegler–Natta catalyst.

The HY and VHY systems employ titanium salts supported on $MgCl_2$ in an active form. Apart from the high yield and isotacticity index, these new catalysts have the great advantage of giving a polymer product with controlled particle size and morphology[3]. The use of these new-generation catalysts has made it possible to simplify the process to only two stages: reaction and separation of the unconverted monomer from the polymer[3].

The present work was undertaken with the aim of obtaining a better understanding of relationships between the catalyst system's molecular structure and properties of iPP polymer.

In order to reach this objective, the molecular characteristics, the crystallization and thermal behaviour of iPP

†To whom all correspondence should be sent.

0032-3861/85/020259-11$03.00

fractions with different isotacticity index, derived from different industrial synthesis processes, were investigated. The investigation was extended to samples obtained after extraction with boiling n-heptane as residues and as soluble extracted fractions.

EXPERIMENTAL

Materials

Five different samples of isotactic polypropylene (iPP), supplied by 'Centro Ricerche G. Natta' Montepolimeri (Ferrara, Italy) were investigated. The characteristics of the samples (obtained by polymerization) are listed in *Table 1*.

Moplen S (MOP-LY) was obtained industrially (hydrocarbon suspension) using a traditional 'low yield' catalytic system (1000 g of polymer g^{-1} of catalyst) based on a $TiCl_3$ catalyst and $AlEt_2Cl$ co-catalyst. The polymer was directly purified in plant from catalytic residues.

Samples of Moplen OP7 (MOP-HY) were prepared in a pilot-plant (hydrocarbon suspension). In this case, a high-yield catalyst system was used consisting of titanium salts grafted on $MgCl_2$ and aluminium alkyl combined with Lewis bases as cocatalysts. Because of the high yield of the reaction (5000 g of polymer g^{-1} of catalyst) the samples of polymer were not purified for catalyst residues. Samples with different isotacticity indices were obtained simply by varying the Al-alkyl/Lewis base ratio.

Moplen OP6 (MOP-VHY) samples were prepared using a third generation high yield catalyst system (superactive). Such a system allows very high catalytic yield (12000 g of polymer g^{-1} of catalyst); the polymer obtained is characterized by a high stereoregularity (no purification is required).

Extraction and dissolution experiments were performed on powder samples of iPP as obtained by polymerization using different solvents. The percentage of material extracted or dissolved together with its viscosity and crystallinity is shown in *Table 2*.

From the data of *Table 1* it emerges that the molecular mass distribution of Mop-LY (97.5), measured by the ratio $\bar{M}_w/\bar{M}_n$, is intermediate between that of Mop-VHY and Mop-HY (97.5) ($\bar{M}_w/\bar{M}_n = 4.69$; 6.01; and 6.74 for Mop-VHY, Mop-LY and Mop-HY respectively).

The rheological behaviour of Mop-LY (97.5) and Mop-HY (97.5) is different; the latter polymers show greater flowability, especially at higher temperature. Consequently the shear stress applied during processing are lower and thus the finished items have less oriented and frozen stresses[3]. Such behaviour, demonstrated by different activation energy of melt flow (10.7 and 9.0 kcal mol^{-1} for HY and LY samples respectively); is likely to be related to diversity in both molecular mass distribution and stereochemical structure of macromolecules.

^{13}C n.m.r. characterization

In order to minimize possible experimental errors, the following procedure was adopted: 80–100 mg of polymer were dissolved in 2 ml of solvent. (Solvent composition: 1,2,4 trichlorobenzene + 15% tetrachlorodideuteroethane (v/v).) All ^{13}C n.m.r. spectra were run at 110°C for at least 24 h with the following parameters: Spectrometer frequency 50.28 MHz; flip angle 45°; relaxation delay 3 s; sweep width 4000 Hz; $N°$ points 16K. Direct *FT* without any line broadening or resolution enhancement.

These conditions were chosen in order to avoid both saturation effects as well as entanglement which may cause line broadening effects. This particular care resulted in a quite noticeable resolution (as shown in *Figure 2*) in which some of the pentads previously observed are clearly split giving heptad resolution. We think that only operating on rather dilute solutions is it possible to achieve high resolution, since it has been previously shown[4] that entangling effects noticeably effect n.m.r. parameters. However, the high dilution forced the use of broad-band decoupling, since NOE was needed in order to improve signal-to-noise ratio. Note that while T_1 values are different within different triads (or pentads), both in polypropylene[5,6] as well as in other polymers[7], no such effect has been reported to date for NOE, probably due to the higher uncertainty on this parameter.

Thus, all integrals of experimental peaks were evaluated without any weighting factor. A computer program was used to simulate resonance patterns arising from configurational sequence multiplicity in the ^{13}C spectra of methyl groups.

In order to evaluate peak areas, graphic integrals were evaluated from each spectrum; appropriate inputs are chemical shifts, linewidth and the assumption of a

Table 1 Characteristics of iPP samples as obtained by polymerization

Sample	Catalytic system	Code	Isotacticity index ^{13}C n.m.r.	Isotacticity index Extraction with n-heptane	$\bar{M}_n$ [a]	$\bar{M}_w$ [a]	$\bar{M}_w/\bar{M}_n$	$[\eta]^{135°C}_{THN}$ [b]	Melt flow index ($g/10^1$)	Crystallinity by X-ray (%)	Melting point (K)
Moplens	Low yield	MOP-LY (97.5)	95.56	97.5	55,066	330,853	6.01	2.35	2.1	64	437
Moplen-OP7-3-4	High yield	MOP-HY (97.5)	95.28	97.5	58,431	393,736	6.74	2.52	1.6	68	436
Moplen OP7-1-2	High yield	MOP-HY (96)	94.87	96.0				2.43	1.8	68	434.5
Moplen OP7-6-7	High yield	MOP-HY (90)	87.89	90.0				2.47	1.6	57	433
Moplen OP6 72–75	Very high yield	MOP-VHY (97.5)	95.13	97.5	71,972	337,489	4.69	2.35		65	436

[a] Values obtained by g.p.c.

[b] Values in tetra-hydro-napthalene

Table 2 Extraction and dissolution action of different solvents on powder samples of iPP as obtained by polymerization some properties of extracted or dissolved fraction are indicated

Solvent Extraction	Fraction extracted or dissolved % (w/w)							$[\eta]^{135°C}_{THN}$		X-ray crystallinity (%)				
	MOP-LY 97.5	MOP-HY 97.5	MOP-HY 96	MOP-HY 90	MOP-VHY 97.5	MOP-LY 97.5	MOP-HY 97.5	MOP-HY 96	MOP-HY 90	MOP-VHY 97.5	MOP-LY 97.5	MOP-HY 97.5	MOP-HY 96	MOP-HY 90	MOP-VHY 97.5
Boiling n-hexane	1.5	–	2.0	–	1.5	0.33	–	0.48	–	0.52	10	–	16	–	24
Boiling n-heptane	2.5	2.5	4.0	10	2.5	0.33	–	0.52	–	0.60	33	–	28	–	33
Boiling iso-octane	3.0	–	4.5	–	2.5	0.33	–	0.53	–	0.48	29	–	33	–	26
Boiling n-octane	32.0	–	35.5	–	27.0	1.19	–	1.08	–	1.36	55	–	55	–	64
Dissolution at 25°C															
Xylene	1.5	2.0	3.6	8.0	4.2	1.03	0.93	1.23	1.45	1.70	–	–	–	–	–
Acetone	0.6	0.4	0.3	0.2	–	–	–	–	–	–	–	–	–	–	–

Lorentzian lineshape as previously used[8]. The best integrals are chosen on a trial-and-error basis in matching observed and computed spectra. This method allows a rather good estimate of integral values (see *Figure 1*).

No attempt was made to interpret the data according to propagation statistics[8,9]. This is due to the possibility that higher stereospecific chains are generated on different sites on the solid catalyst surface[10,12]. Moreover, since different molecular weight distributions are present in our samples, the hypothesis that materials formed by different mechanisms are present seems reasonable.

Radial growth rate of spherulite by optical microscopy

A Reichert polarizing optical microscope equipped with a Mettler hot stage was used for determining the radial growth rates G of iPP spherulites isothermally crystallizing at different crystallization temperature T_c. The hot stage could be held at a fixed temperature within $\pm 0.2°C$.

The following procedure was used: iPP films were sandwiched between a microscope slide and a cover glass, heated at 190°C and kept at this temperature for 10 min to destroy any trace of crystallinity, then the temperature was rapidly lowered to a pre-fixed T_c and the iPP samples allowed to crystallize isothermally.

Photomicrographs of growing spherulites were taken at appropriate time intervals. The radii of spherulites 'r' were measured from the photomicrographs and G calculated as the slope of the linear plots of r as a function of time.

Overall kinetic rate constant by differential scanning calorimetry (d.s.c.)

The kinetics of isothermal crystallization from melt of all samples were studied by using a Perkin–Elmer DSC-2 differential scanning calorimeter operating under N_2 atmosphere. The following procedure was employed: the samples were kept for 10 min at 190°C and then rapidly cooled to the crystallization temperature T_c.

The heat (dH/dt) evolved during the isothermal crystal-

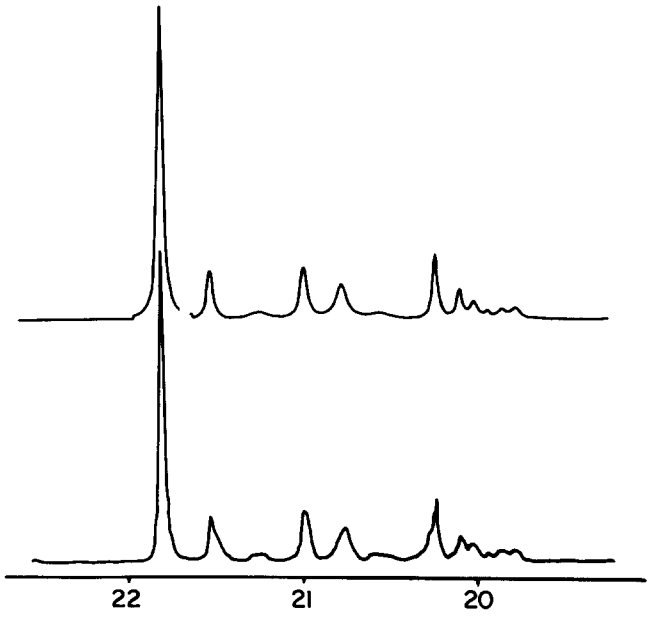

Figure 1 50.28 MHz, ^{13}C n.m.r. spectrum of the boiling heptane soluble fraction of Mop–HY(97.5); top calculated, bottom experimental. Only the methyl region of the spectrum is shown

lization was recorded as function of time t and the weight fraction x_t of material crystallized after the time t was determined from the relation:

$$X_t = \int_0^t (dH/dt) / \int_0^\infty (dH/dt)/dt$$

where the first integral is the crystallization heat evolved at the time t and the second integral is the total crystallization heat for $t = \infty$.

The melting temperature T'_m and the apparent enthalpy of fusion ΔH^*_f of each sample after isothermal crystallization at T_c were measured from the maxima and the areas (respectively) of d.s.c. endotherms obtained by heating the samples directly from T_c to T'_m with heating rates of 20°C min^{-1}. Higher scan rates (40°, 80°C min^{-1}) were also used in order to check the influence of the heating rate on the shape of the melting endotherm. The temperatures of the calorimeter were calibrated against the melting points of high purity standards under different heating conditions with a precision of ±0.2 degrees.

The crystallinity fraction X_c of the samples was determined at each T_c by the ratio of ΔH^*_f to the fusion enthalpy ΔH_f of a sample with 100% of crystallinity, taken as 50 cal g^{-1} (209 kJ kg^{-1})[13].

WAXS measurements

Wide angle X-ray scattering (WAXS) measurements were carried out on a (PW 1050 MODEL) Philips powder diffractometer (CuKα Ni-filtered radiation) to evaluate both the crystallinity index and the content of β form of iPP.

RESULTS AND DISCUSSION

Results of ^{13}C n.m.r. spectral analysis

The results of ^{13}C n.m.r. spectral analysis are summarized in *Table 3*. From the data in this Table some clear conclusions can be drawn.

(i) The most stereoregular polymer is Mop-LY (97.5), which has the highest isotacticity index both in the as obtained by polymerization material (type A samples), as well as in the boiling heptane insoluble fraction (type B samples).

(ii) Polymers prepared with the high yield catalyst show a pentad distribution which approximately follows the tacticity index. This holds for both type A and B samples as well as for boiling heptane soluble fractions (type C samples).

(iii) Mop-LY (97.5) and to a lesser extent Mop-VHY (97.5) boiling heptane soluble fraction are less stereoregular. This observation implies that the more stereoregular polymer has the less stereoregular heptanic extract.

(iv) While we do not wish to over-estimate pentad distribution in our samples, due to the lack of a statistical analysis, it seems necessary to point out the noticeable value of the intensity of pentad mrmr both in Mop-LY (97.5) and in its boiling heptane insoluble fraction compared to all other high-yield polypropylenes.

There is a similarity between Mop-VHY (97.5) and Mop-LY (97.5) as regards the tacticity values of the heptanic extract and also the pentad distribution. Finally, the heptad at 19.80 ppm, intense in all boiling heptane

Table 3 Normalized integrals* of sterical configurational pentad

Pentads	Frequency	Heptanic residues					Samples as obtained by polymerization					Heptanic extracts				
		LY97.5	VHY97.5	HY97.5	HY96	HY90	LY97.5	VHY97.5	HY97.5	HY96	HY90	LY97.5	VHY97.5	HY97.5	HY96	HY90
mmmm	21.80	929.6	930.1	921.6	895.0	893.5	892.0	912.0	895.2	892.0	760.0	370.6	396.4	486.4	442.3	419.6
mmmr	21.54	15.4	16.4	19.7	39.8	29.1	23.8	19.8	30.7	26.7	57.8	87.5	94.2	90.7	112.0	104.6
rmmr	21.15	6.0	5.4		5.5	2.0	9.8	5.8	7.7	7.7	8.9	41.4	49.2	35.7	35.8	
mmrr	21.01	14.9	16.4	33.3	33.3	31.2	28.0	20.1	30.7	26.7	66.7	103.1	102.4	93.0	98.5	126.8
mrmm	20.78	6.0	8.2	6.2	9.3	9.0	25.2	7.3	7.7	16.7	22.2	119.7	110.6	85.5	85.1	88.7
rmrr																
mrmr	20.53	11.3	2.2			1.0	7.0			1.3	15.5	36.8	24.6	26.0	31.3	31.0
	20.47															
rrrr	20.25	6.0	8.8	6.9	5.9	20.5	5.6	16.4	6.1	9.8	28.9	101.3	90.1	81.8	80.6	86.9
	20.11															
rrrm	20.04	3.5	6.5	2.5		2.4	2.1	7.9	3.1	6.6	13.3	81.1	70.4	47.6	55.5	53.2
	19.96															
mrrm	19.38	7.0	7.1	9.4	11.1	11.0	6.3	9.4	9.2	12.4	26.7	67.9	62.3	57.5	59.1	53.2
	19.80															
Isotacticity index[b]		967.1	965.3	961.1	960.9	945.7	955.6	951.3	952.8	948.7	878.9	629.3	658.6	715.0	697.5	682.9

[a] ppm from TMS for 1000 atoms of C
[b] Isotacticity index = mm+1/2mr . 1000

soluble fractions, is completely missing in all insoluble fractions, where the other heptad, at 19.88, belonging to the same pentad mrrm is always present, see *Figure 2*.

Thus, the observation of Doi *et al.*[10] that '*polypropylenes produced with the supported catalyst system are a mixture of macromolecules of different stereoregularities, indicating that active sites having different stereoregulating capabilities are present in the catalyst*' is confirmed by our data and holds also for unsupported Ziegler–Natta catalyst.

Doi *et al.* indicated for highly stereoregular fractions the following relationships: $mmr \simeq mmrr = 2|mrrm|$. This relationship is approximately verified on Mop-LY (97.5) and Mop-VHY (97.5) residues (in which, however, a high content of rrrr was found), but it is not verified for Mop-HY (97.5), (96) and (90), where $mrrm \simeq 1/3$ mmrr. Again the different pentad relationships supports the view of the existence of catalytic sites with different stereoregulating capability[11,12].

Melt crystallization

Radial growth rate of spherulites. The values of the radial growth rate G of thin films of iPP as obtained from polymerization (type A samples) and of residues after extraction with boiling n-heptane (type B samples) are listed in *Table 4* as a function of crystallization temperature T_c. It can be observed that, for a given sample, G decreases with increase in T_c (at least for the range of T_c explored). In the case of high yield samples it is found that G, for both samples A and B, increases with the increase of the isotacticity index (I.I.).

For a given T_c the values of G of type B samples are larger than those of sample A. This last finding may be accounted for by assuming that boiling n-heptane is able to extract selectively less stereoregular and/or amorphous fractions of iPP. Such fractions (compatible in the melt with the most stereoregular fraction) act as a diluent depressing the radial growth rate of spherulite of type A samples[12,14].

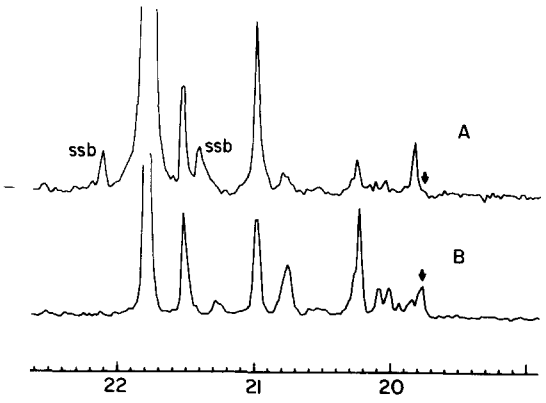

Figure 2 50.28 MHz, ^{13}C n.m.r. spectra of Mop–HY(97.5): (a) boiling point heptane insoluble fraction; (b) boiling heptane soluble fraction. The arrow denotes the heptad missing in the heptanic residue and present in the heptanic extract on the next neighbouring peak the situation is reversed

A comparison, at constant T_c, for samples with higher I.I. shows that Mop-LY (97.5) and Mop-HY (97.5) have similar G whereas Mop-VHY (97.5) is characterized by higher values of the spherulite growth rate; the difference being larger for the type B samples (see *Table 4*).

Overall kinetics of crystallization. Plots of the half time of crystallization $t_{0.5}$ *versus* T_c are shown in *Figures 3a* and *b* for sample A and B, respectively. From the examination of the trends of the plots the following emerges:

(i) In the case of sample belonging to the HY series the values of $t_{0.5}$ for a given T_c decrease (both for type A and type B) with increase of the isotacticity index.

(ii) In both samples A and B, Mop-VHY (97.5) has values of $t_{0.5}$ that are higher than those of Mop-LY (97.5).

(iii) Irrespective of its high isotacticity index Mop-LY (97.5), shows values of $t_{0.5}$ that at constant T_c are lower than those of HY and VHY iPP. Such behaviour is more accentuated in the case of type A samples and at higher T_c.

(iv) Type A samples of Mop-LY (97.5) and Mop-VHY (97.5) are characterized by values of $t_{0.5}$, at a given T_c, that are lower than those of sample B (see *Table 5*).

The variation of $t_{0.5}$ with the undercooling $\Delta T = T_m - T_c$, where T_m is the equilibrium melting temperature of each iPP sample, is shown in *Figures 4a* and *b* for samples A and B respectively. Type A samples belonging to the high yield series show values of $t_{0.5}$ that, for a given ΔT, increase with increases in the isotacticity index.

At the same value of ΔT Mop-LY (97.5) (sample A) is characterized by values of $t_{0.5}$ considerably lower than those of high yield series and of very high yield iPP.

In the case of type B samples it can be noticed that, for the same ΔT, Mop-LY (97.5) has values of $t_{0.5}$ lower than those of Mop-HY (97.5) and Mop-VHY (97.5) but comparable with those of Mop-HY (90).

The number of primary nuclei per unit volume ($\bar{N}$), as a function of T_c, is reported, for each iPP sample, in *Table 6*. The values of $\bar{N}$ have been obtained by using the following relation:

$$Kn = \frac{4}{3}\pi G^3 \frac{\rho_c}{\rho_a(1-\lambda)}\bar{N} \qquad (1)$$

where ρ_c and ρ_a are the density of crystalline and amorphous regions, respectively and λ is the fraction of crystallized material at $t = \infty$. Equation (1) is valid for the assumption of a three dimensional spherical growth with instantaneous nucleation[15].

The figures of *Table 6* show that type A sample of Mop-LY (97.5) is characterized by the largest values of $\bar{N}$. This

Table 4 Radial growth rate (G) of iPP spherulites as function of crystallization temperature T_C (°C). (Figures in brackets refer to type *B* samples: the others to type *A* samples; G is given in μ/min)

Sample	T_C (°C) 128		129		131		132	
Mop-LY (97.5)	8.50	(9.00)	7.00	(7.20)	4.45	(4.75)	3.70	(3.80)
Mop-HY (97.5)	8.35	(9.40)	7.25	(7.70)	5.05	(5.07)	4.03	(4.03)
Dop-HY (96)	7.10	(8.80)	5.70	(6.85)	3.68	(4.25)	3.05	(3.40)
Mop-HY (96)	6.75	(7.37)	5.26	(6.05)	3.25	(3.82)	2.60	(2.95)
Mop-VHY (97.5)	9.10	(11.2)	7.25	(9.15)	4.77	(6.25)	3.85	(5.75)

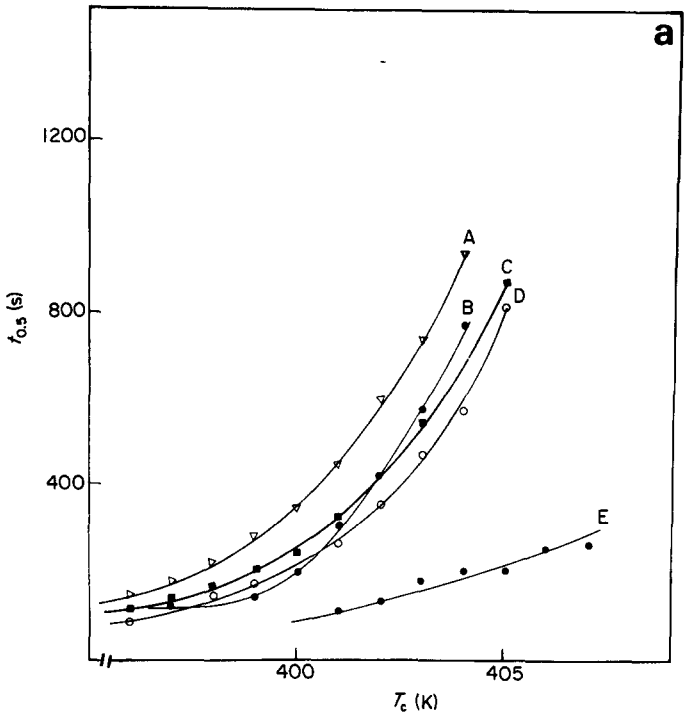

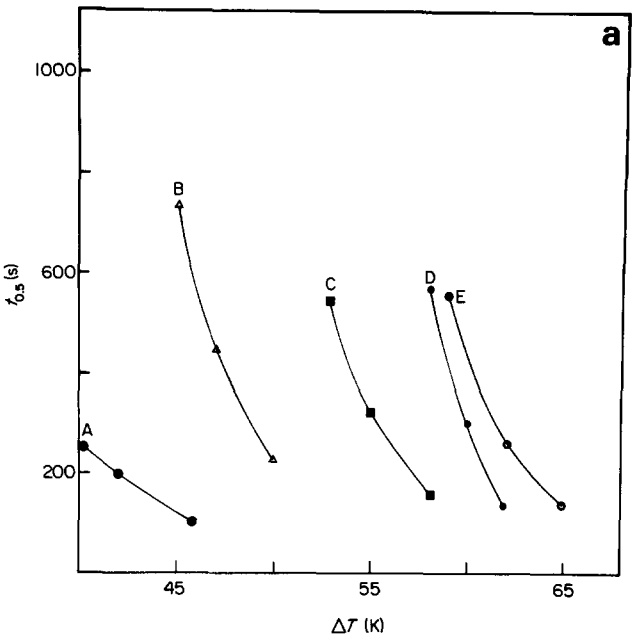

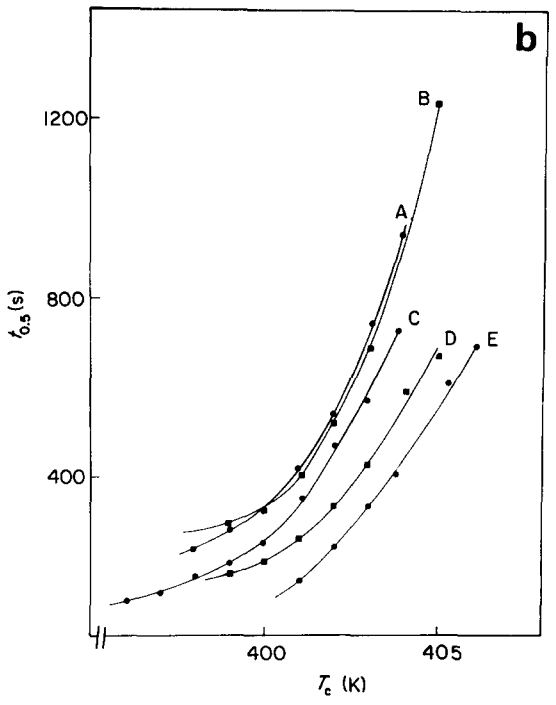

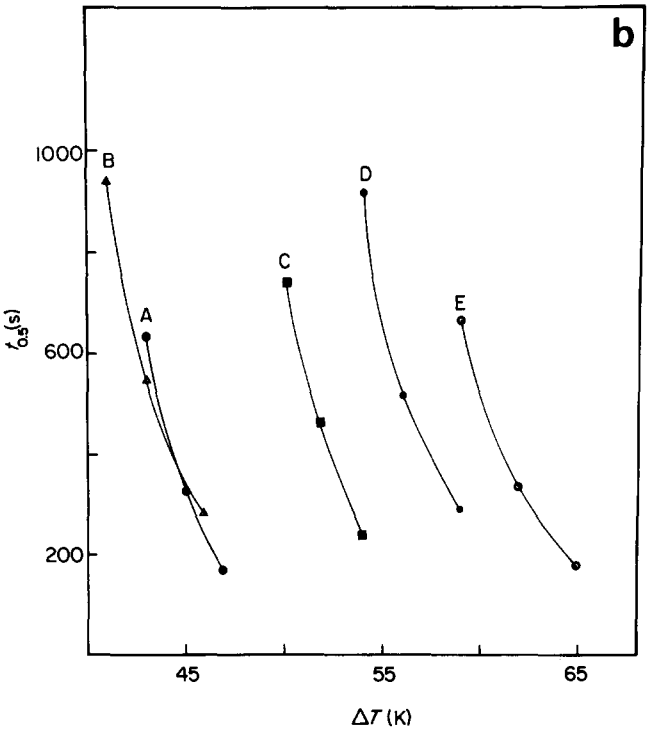

Figure 3 Half time of crystallization $t_{0.5}$ (s) as a function of crystallization temperature T_c for: (a) iPP samples as obtained by polymerization (type A); (b) iPP samples after extraction with boiling n-heptane (type B). Curve A: HY 90; curve B: VHY 97.5; curve C: HY 96; curve D: HY 97.5; curve E: LY 97.5

Figure 4 Half time of crystallization $t_{0.5}$ (s) as a function undercooling $\Delta T = T_m - T_c$ for (a) iPP samples as obtained by polymerization (type A) (b) iPP samples after extraction with boiling n-heptane (type B)

Table 5 Half-time of crystallization ($t_{0.5}$ in s) as function of crystallization temperature T_c. (Figures in brackets refer to type B iPP samples, the others to type A samples)

Sample	T_c (°C) 128		129		131		132	
MOP-LY (97.5)	100	(162)	120	(243)	197	(393)	201	(639)
MOP-HY (97.5)	262	(262)	350	(332)	570	(595)	802	(672)
MOP-HY (96)	325	(333)	415	(470)	683	(741)	875	–
MOP-HY (90)	450	(415)	600	(550)	940	(943)	–	–
MOP-VHY (97.5)	300	(379)	420	(520)	770	(925)	–	(1244)

Table 6 Number of primary nuclei per unit volume (cm^3) (N) as function of crystallization temperature T_C (°C). (Figures in brackets refer to type B samples; others to type A samples)

Sample	T_C (°C) 128		132		135	
Mop-LY 97.5	1.9×10^7	(2.8×10^6)	3.3×10^7	(6.7×10^5)	5.3×10^7	–
Mop-HY 97.5	1.1×10^6	(1.4×10^6)	2.8×10^5	(6.1×10^5)	6.3×10^5	–
Mop-HY 96	5.5×10^5	(9.5×10^5)	2.6×10^5	(6.4×10^5)	9.0×10^5	–
Mop-HY 90	3.7×10^5	(5.6×10^5)	4.1×10^5	(4.5×10^5)	3.9×10^5	–
Mop-VHY 97.5	7.0×10^5	(1.3×10^5)	2.9×10^5	(2.8×10^4)	–	–

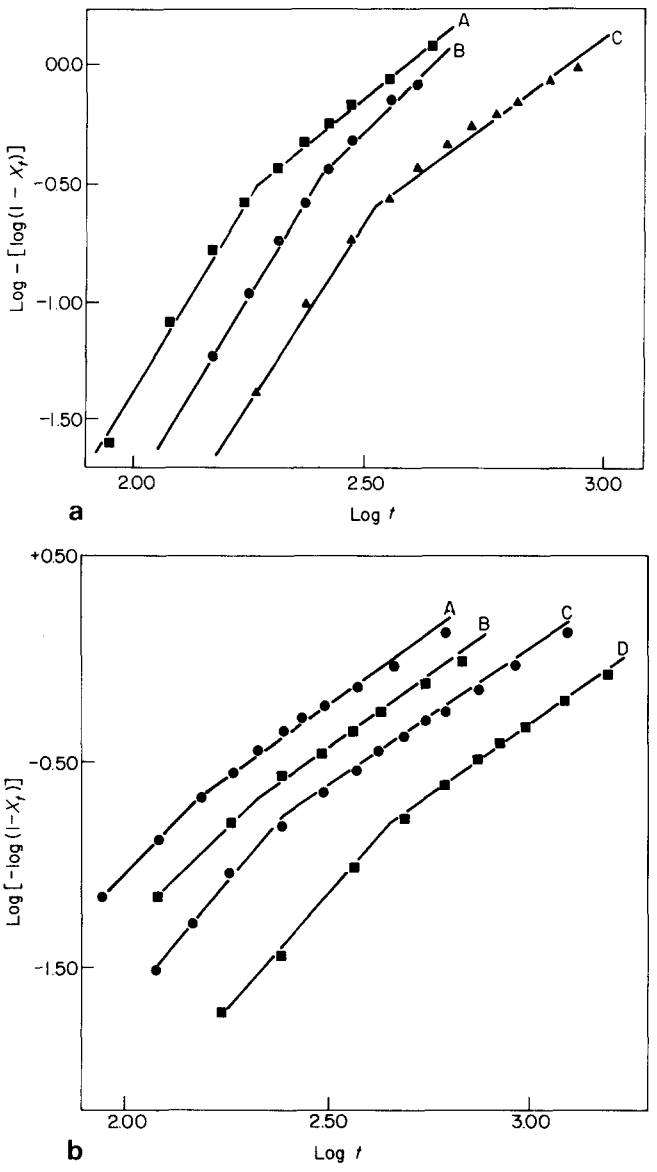

Figure 5 Avrami plots for: (a) Mop-LY (97.5) samples A. Curve A: 401°C; curve B: 405°C; curve C: 407°C (b) Mop-LY (97.5) samples B. Curve A: 401°C; curve B: 402°C; curve C: 403°C; curve D: 405°C

finding explains the high overall rate of crystallization (low $t_{0.5}$) observed for such material.

It can be observed further that samples of Mop-LY (97.5) and Mop-VHY (97.5) as obtained by polymerization have values of $\bar{N}$, at a given T_c, markedly higher than those of corresponding samples insoluble in boiling n-heptane.

This is in agreement with the lower overall rate of crystallization showed by type B sample of the two iPP polymers.

The analysis of the crystallization kinetics, for each T_c, has been carried out on the basis of the Avrami equation[15]:

$$1 - X_t = \exp(-Knt^n) \quad (2)$$

where Kn ($= \ln 2/t^n_{0.5}$) is the kinetic rate constant and 'n' is a parameter dependent on the type of primary nucleation and on the geometry of growing crystals. In the case of samples of type A and B of iPP belonging to the high yield series and to Mop-VHY (97.5), plots of $\log[-\log(1 - X_t)]$ *versus* $\log t$ are linear for all T_c investigated even at high conversion time. However, as shown by *Figures 5a* and *b*, an abrupt change in the slope of the Avrami plots is observed in the case of samples of type A and B of Mop-LY (97.5) at well defined values of the conversion times.

This behaviour is probably related to a primary and a secondary process of crystallization at lower and higher times of conversion respectively.

Values of K_n and n have been calculated, for all T_c investigated, from the intercept and the slope of the Avrami lines (see *Table 7*).

In the case of Mop-LY (97.5) two set of values have been derived corresponding to the primary and secondary crystallization. Samples A and B show values of the Avrami index n in the range 2.0–2.9. This suggests a process of crystallization characterized by a heterogeneous nucleation and by a three dimensional growth of crystals[15].

In the case of the secondary crystallization process, observed for Mop-LY (97.5), at higher times of conversion, n assumes values in the range 1.0–1.4 typical of a one-dimensional growth of crystalline entities.

Phenomena of secondary crystallization were already observed by one of us in the case of less stereoregular fraction of iPP sample[2]. In this case, samples of iPP were prepared in the laboratory by using a Ziegler–Natta catalyst. Fractions with different stereoregularity were obtained by successive extractions with hydrocarbon solvents or by isothermal fractional crystallization and characterized in terms of stereochemical pentad population by ^{13}C n.m.r. analysis.

The secondary process of crystallization was mainly ascribed to the fact that less perfect molecules, after a certain time of crystallization, start to crystallize in interlamellar regions giving rise to the formation of less perfect crystals.

The results reported in the present paper cannot be explained in terms of different isotacticity index as Mop-LY (97.5) show a I.I. value comparable with that of Mop-HY (97.5) and Mop-VHY (97.5) and higher than those of

Table 7 Half time of crystallization $t_{0.5}$, Avrami index n and overall kinetic rate constant K_n of iPP samples as function of crystallization temperature (Values in brackets refer to type B samples; asterisks indicate values corresponding to secondary crystallization process).

Mop – LY (97.5)

T_c (K)	$t_{0.5}$ (s)		n		K_n (s^{-n})			
401	100	(162)	2.5; 1.3*	(2.1); (1.4*)	$6.9\ 10^{-6}$	$1.7\ 10^{-3}$*	$(1.6\ 10^{-5})$	$(5.6\ 10^{-4}$*)
402	124	(243)	–	(2.0); (1.4*)			$(1.2\ 10^{-5})$	$(3.2\ 10^{-4}$*)
403	174	(334)	2.0; 1.0*	(2.3); (1.4*)	$2.3\ 10^{-5}$	$4.0\ 10^{-3}$*	$(1.1\ 10^{-6})$	$(2.0\ 10^{-4}$*)
404	195	(393)	2.3; 1.5*	(2.2); (1.4*)	$3.7\ 10^{-6}$	$2.5\ 10^{-4}$*	$(1.4\ 10^{-6})$	$(1.6\ 10^{-4}$*)
405	197	(639)	2.3; 1.7*	(2.2); (1.4*)	$3.7\ 10^{-6}$	$8.7\ 10^{-5}$*	$(4.7\ 10^{-7})$	$(8.2\ 10^{-5}$*)
406	252	(688)	2.2; 1.6*	(2.3); (1.4*)	$3.6\ 10^{-6}$	$9.9\ 10^{-5}$*	$(2.1\ 10^{-7})$	$(7.4\ 10^{-5}$*)
407	260	–	2.0; 1.0*	–	$1.0\ 10^{-5}$	$2.7\ 10^{-5}$*	–	–

Mop – HY (97.5)

T_c (K)	$t_{0.5}$ (s)		n		K_n (s^{-n})	
396	76	–	2.5	A	$1.3\ 10^{-5}$	–
397	105	–	2.4	–	$9.8\ 10^{-6}$	
398	134	–	2.5	–	$3.3\ 10^{-6}$	–
399	165	(179)	2.5	(2.7)	$2.0\ 10^{-6}$	$(5.7\ 10^{-7})$
400	189	(207)	2.5	(2.6)	$1.4\ 10^{-6}$	$(6.6\ 10^{-7})$
401	262	(262)	2.5	(2.9)	$6.2\ 10^{-6}$	$(6.7\ 10^{-7})$
402	352	(732)	2.5	(2.9)	$3.0\ 10^{-7}$	$(3.4\ 10^{-8})$
403	471	(430)	2.5	(2.8)	$2.5\ 10^{-7}$	$(2.9\ 10^{-8})$
404	572	(595)	2.3	(2.6)	$3.2\ 10^{-7}$	$(4.2\ 10^{-8})$
405	810	(672)	2.5	(2.6)	$3.6\ 10^{-8}$	$(3.1\ 10^{-8})$

MOP – HY (96)

T_c (K)	$t_{0.5}$ (s)		n		K_n (s^{-n})	
396	105	–	2.0	–	6.3×10^{-5}	–
397	133	–	2.1	–	2.4×10^{-5}	–
398	163	–	2.1	–	1.6×10^{-5}	–
399	197	–	2.1	–	1.1×10^{-5}	
400	239	(241)	2.0	(2.6)	1.0×10^{-5}	(4.4×10^{-7})
401	325	(353)	2.2	(2.5)	1.2×10^{-6}	(3.0×10^{-7})
402	–	(470)	–	(2.6)	–	(1.1×10^{-7})
403	542	(572)	2.4	(2.7)	1.9×10^{-7}	(2.5×10^{-8})
404	–	(741)	–	(2.6)	–	(2.5×10^{-8})
405	873	–	2.4	–	6.0×10^{-8}	–

Mop – HY (90)

T_c (K)	$t_{0.5}$ (s)		n		K_n (s^{-n})	
396	139	–	2.2	–	1.3×10^{-5}	–
397	173	–	2.3	–	4.9×10^{-6}	–
398	218	–	2.4	–	1.7×10^{-6}	–
399	285	(283)	2.5	(2.5)	5.0×10^{-7}	(5.1×10^{-7})
400	344	(317)	2.4	(2.6)	5.7×10^{-7}	(2.2×10^{-7})
401	450	(415)	2.6	(2.7)	8.8×10^{-7}	(5.9×10^{-8})
402	603	(550)	2.5	(2.8)	7.8×10^{-8}	(2.1×10^{-8})
403	740	(749)	2.5	(2.7)	4.6×10^{-8}	(1.2×10^{-8})
404	940	(943)	2.4	–	5.1×10^{-8}	–

Mop – VHY (97.5)

T_c (K)	$t_{0.5}$ (s)		n		K_n (s^{-n})	
397	107	–	2.3	–	1.5×10^{-5}	–
399	135	(287)	2.5	(2.6)	3.3×10^{-6}	(2.8×10^{-7})
400	190	–	2.9	–	1.7×10^{-7}	–
401	304	(397)	2.8	(2.1)	7.7×10^{-8}	(2.7×10^{-6})
402	420	(520)	2.8	(2.3)	3.1×10^{-8}	(3.9×10^{-7})
403	577	(686)	2.8	(2.4)	1.3×10^{-8}	(1.1×10^{-7})
404	770	(925)	2.9	(2.5)	3.0×10^{-9}	(2.7×10^{-8})
405	–	(1244)	–	(2.5)	–	(1.3×10^{-8})

Table 8 Observed melting temperature (K) as function of crystallization temperature for iPP samples as obtained by polymerization and extraction residues

	Moplen-LY (97.5)		Moplen-HY (97.5)		Moplen-HY (96)		Moplen-Hy (90)		Moplen-VHY (97.5)	
T_c (K)	A	B	A	B	A	B	A	B	A	B
395	437					435.5				
396			437	437	435	436	434	435		
397	437		437	438	436	436	434		436	
398			437.5	438	436	436	434	435	436	
399	438		438	438	437	437	435	435	437	438
400		437	438	439	437	437	435	435	437	439
401	438	437	438.5		437	437	435	436	438	439
402		437.5	439	439	437	438	436	436	438	439
403	438	438	439	439	438	438	436	436	439	440
404		438	440	439	438	438	436		439	440
405	439	438.5								440
406										
407	440									
408										

[A] Samples as obtained by polymerization
[B] Samples obtained as residue after extraction with boiling n-heptane

Table 9 Values of the equilibrium melting temperature T_m and of constant γ for the various samples of iPP

		iPP as obtained by polymerization		iPP residues	
Sample	Isotacticity index (%)	T_m (K) (±3)	γ	T_m (K) (±3)	γ
Moplen LY 97.5	97.5	447	5.6	448	4.5
Moplen HY 97.5	97.5	463	2.6	464	2.6
Moplen HY 96	96.0	456	2.9	454	3.1
Moplen HY 90	90.0	448	3.8	445	3.6
Moplen VHY 97.5	97.5	461	2.6	458	3.4

other high yield samples for which no secondary processes of crystallization are observed.

Melting behaviour. D.s.c. thermograms of isothermally crystallized high and very high yield samples, present only one fusion peak irrespective of heating rate and crystallization temperature. Conversely, the thermograms of Mop-LY (97.5) generally show a broad fusion peak with a shoulder at lower temperatures. As shown by the data of *Table 8* samples of iPP as obtained by polymerization (type A) and corresponding samples obtained as residues after extraction with boiling n-heptane (type B) crystallized isothermally at the same T_c, are characterized by practically coincident values of the observed T_m' melting temperature; small differences are in the range of experimental errors.

The T_m' of the various samples increases linearly with T_c according to the relation

$$T_m' = T_m \frac{(\gamma - 1)}{\gamma} + T_c/\gamma \qquad (3)$$

where T_m is the equilibrium melting temperature and γ is a constant determined by the ratio between the final thickness of the crystalline lamellae of the spherulites crystallized at T_c after a certain time and the initial critical thickness[16]. The values of T_m and γ calculated by extrapolation of the $T_m' \rightarrow T_c$ lines to the line of equation $T_m' = T_c$ and from the slopes, respectively, are reported, for all samples, in *Table 9*.

In the case of type A of high yield iPP samples the values of T_m decrease with decreases in the isotacticity index.

The T_m of type A and B of Moplen-LY are lower than those of samples having comparable isotacticity index. It is interesting to note that, for a given T_c, the T_m' of Mop-LY are close to those of Mop-HY (97.5) and Mop-VHY (97.5), whereas the values of γ are larger (see *Tables 8* and *9*). The latter observation suggests that the thickening process of the lamellae ($\gamma > 1$) during the crystallization at T_c is much more pronounced in the case of Mop-LY iPP. As shown by *Table 9*, type A and B samples of corresponding iPP have almost the same T_m.

Melting d.s.c. endotherms of type A Mop-LY (crystallized isothermally at $T_c = 401$ K for different times of crystallization) are shown in *Figure 6*. It can be observed that the shoulder at lower temperature becomes distinct and clearly resolved only after larger times of crystallization; i.e. when a secondary process of crystallization predominates (compare the times of *Figure 6* with the Avrami plots of *Figure 5*). This observation supports the hypothesis that material with different structure and morphology crystallizes during the process of primary and secondary crystallization of the polymer. The anomalous large γ value of Mop-LY (97.5) nevertheless indicates that phenomena of perfectioning of existing crystals following an annealing at T_c may also play an important role in determining the secondary crystallization process in this polymer.

The presence along the chains of Mop-LY (97.5) of a larger amount of configurational defects of mrmr type (see ^{13}C n.m.r. analysis) is likely to increase the mobility of the macromolecules in the crystal and on its surface making the processes of refolding and recrystallization easier during annealing at T_c.

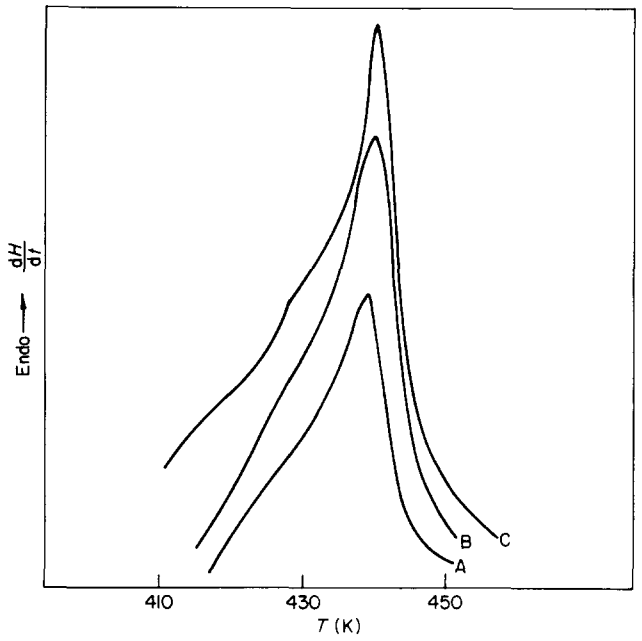

Figure 6 D.s.c. melting endotherms for Mop-LY (97.5) iPP isothermally crystallized at 401 K after different times of crystallization. Curve A: after 70 s; curve B: after 155 s; curve C: after 600 s

Nucleation control of crystallization rate. Assuming that the process of crystal growth (corresponding to the primary crystallization) is controlled by a mechanism of surface coherent bidimensional secondary nucleation, then, in accordance with the kinetic theory of polymer crystallization[17], the temperature dependence of G and K_n is given by relations (4a) and (4b).

$$\log_{10}G=\log_{10}G_0-\frac{\Delta F^*}{2.3RT}-\frac{\Delta\Phi^*}{2.3KT_c} \tag{4a}$$

$$\frac{1}{n}\log_{10}K_n=A_0-\frac{\Delta F^*}{2.3RT_c}-\frac{\Delta\Phi^*}{2.3KT_c} \tag{4b}$$

where G_0 and A_0 are constant (assuming that the density of primary nucleation at each T_c examined does not vary with time); ΔF^* is the activation energy for the transport of the molecules at the liquid–solid interface; K is the Boltzmann constant and $\Delta\Phi^*$ is the energy of formation of a nucleus of critical dimensions, expressed as:

$$\Delta\Phi^*=\frac{4b_0\sigma\sigma_e T_m}{\Delta H_f\Delta T} \tag{5}$$

In equation (5) b_0 is the distance between two adjacent fold planes, σ and σ_e are the free energy of formation per unit area of the lateral and folding surfaces of the crystals and ΔH_f is the enthalpy of fusion.

The transport term ΔF^* is usually expressed as the activation energy of the viscous flow according to the relation of Williams, Landel and Ferry[16]:

$$\Delta F^*=\frac{C_1T_c}{C_2+T_c-T_g} \tag{6}$$

where C_1 and C_2 are constants generally assumed equal to 4.12 kcal mol^{-1} (17.2 kJ mol^{-1}) and 51.5 K respectively and T_g is the glass transition temperature. For all the samples examined $T_g=260$ K has been used according to the literature data.

Plots of $1/n\log_{10}K_n+\Delta F^*/(2.3RT_c)$ and $\log_{10}G+\Delta F^*(2.3RT_c)$ *versus* $T_m/(T_c\Delta T)$ are straight lines whose slopes, according to equations (4) and (5), are given by the quantity:

$$\frac{4b_0\sigma\sigma_e}{2.3K\Delta H_f} \tag{7}$$

substituting $b_0=0.525$[19], $\Delta H_f=209$ kJ/kg[13] and $\sigma=0.1$ ($b_0\Delta H_f$) into equation (7), the surface energy of folding σ_e of iPP lamellar crystals and the free energy of formation of a nucleus of critical dimensions $\Delta\Phi^*$ were calculated.

Samples of type A and B of HY and VHY iPP show values of σ_e and $\Delta\Phi^*$ that increase with increases in the isotacticity index, i.e. the data points are interpolated by the same curves (see *Figures 7* and *8*).

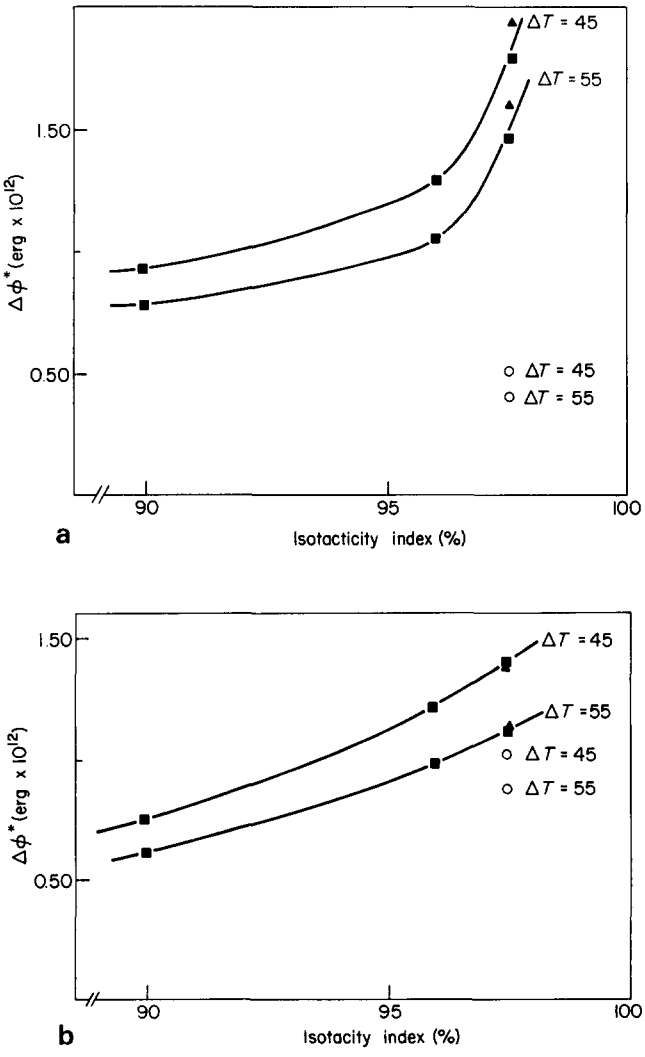

Figure 7 Free energy of formation of a nucleus of critical dimension $\Delta\Phi^*$ *versus* the isotacticity index (I.I) for two different values of the undercooling ΔT: (a) type A samples of iPP (b) type B samples of iPP. (○) LY; (■) HY; (▲) VHY (from $1/n\log K_n+\Delta F^*//(2.3RT_c)$ *versus* $T_m/\Delta T\,T_c$ plots)

It can be observed that σ_e and $\Delta\Phi^*$ are, in the case of Mop-LY, lower than those of HY and VHY samples with comparable isotactacity index. As shown in *Figures 7* and *8*, type A samples are characterized by higher values of σ_e and $\Delta\Phi^*$.

It is interesting to point out that the trend of the data points of *Figure 8* is very similar to that observed when the values of the equilibrium melting temperature are plotted against the isotacticity index (see *Figure 9*).

The trend observed in σ_e and $\Delta\Phi^*$ is probably accounted for by the amount and distribution of configurational irregularities existing along the molecules of the various samples and by the molecular weight distribution as a consequence of the different catalyst systems employed (see *Tables 1* and *2*). The large variation observed in the values of σ_e of high yield samples can probably be ascribed to the fact that the fold surface of iPP crystals undergoes profound changes and becomes less regular as the content of stereoirregular sequences in the chains and/or the presence of uncrystallizable polymer increases.

Moreover, it is interesting to underline that a similar trend in $\Delta\Phi^*$ has also been observed in the melt crystallization of isotactic-(propylene-1, butene) random copolymers[19] and for iPP fractions with different degrees of stereoregularity[2]. In fact $\Delta\Phi^*$ was found to decrease with increases in the butene content or with decrease in the isotactic pentads concentration.

The trend observed in *Figure 7* for $\Delta\Phi^*$ is in agreement with the results shown by *Figure 4*. Thus, the increase of the overall rate of crystallization, with decreases in the isotacticity index found, at a given ΔT, in the case of HY polymers may be ascribed to the corresponding lowering in the values of the free energy of formation of a nucleus of critical dimensions. Plots of $1/n \log_{10} K_n + \Delta F^*/(2.3RT_c)$ *versus* $T_m/T_c\Delta T$ are also linear in the case of the secondary crystallization process observed for Mop-LY type A and B samples. The values of $\Delta\Phi^*$ and σ_e calculated are practically coincident with those corresponding to the primary crystallization. This result indicates that during the two processes similar lamellar crystals are involved. This observation strongly suggests that (for Mop-LY samples at least) and under our conditions of crystallization the secondary crystallization is most probably accounted for by a process of annealing at T_c in agreement with the larger γ values found for this polymer.

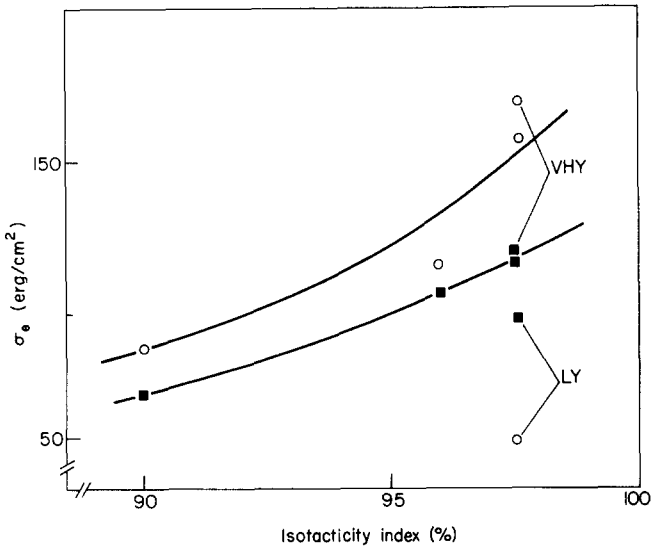

Figure 8 Surface free energy of folding δ_e as function of isotacticity index for type A and B iPP. (○ type A samples; ■ type B samples

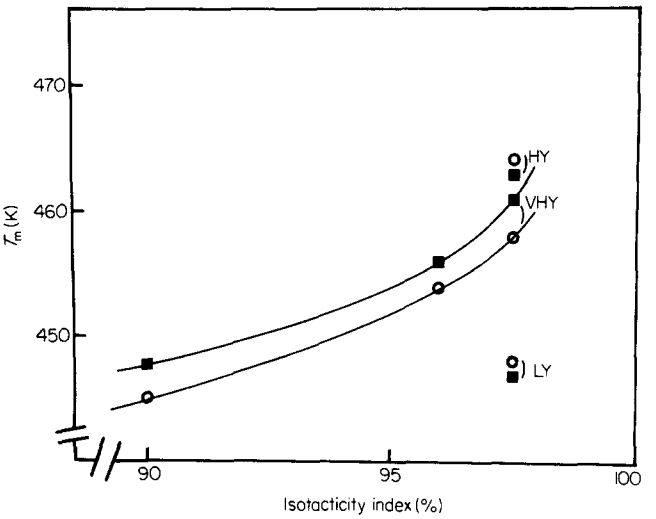

Figure 9 Plots of T_m *versus* I.I. for type A and B of iPP. (■: type A samples; ○: type B samples)

ACKNOWLEDGEMENT

This work was partly supported by 'Progetto Finalizzato Chimica Fine' of Italian C.N.R.

REFERENCES

1 Martuscelli, E., Pracella, M. and Zambelli, A. *J. Polym. Sci. Polym. Phys. Edn.* 1980, **18**, 619
2 Martuscelli, E., Pracella, M. and Crispino, L. *Polymer* 1983, **24**, 693
3 Galli, P. 28th IUPAC MACRO Symposium, July 1982, Amherst, Mass., USA
4 Stilbs, P., Mosely, M. E. *Polymer* 1981, **22**, 321
5 Imoue, Y., Nishioka, A. and Chuio, R. *Makromol. Chem.* 1973, **168**, 163
6 Randall, J. C. *J. Polym. Sci. Polym. Phys. Edn.* 1976, **14**, 1693
7 Schilling, F. C. *Macromolecules* 1978, **11**, 1290
8 Cais, R. E. and Bovey, F. A. *Macromolecules* 1977, **10**, 752
9 Frish, H. L., Mallows, C. L. and Bovey, F. A. *J. Chem. Phys.* 1966, **45**, 1565
10 Doi, Y., Suzuki, E. and Keii, T. *Makromol. Chem. Rapid Comm.* 1981, **2**, 293
11 Corradini, P., Barone, V. and Guerra, G. *Macromolecules* 1982, **15**, 1242
12 Segre, A. L., Delfini, M., Paci, M. and Raspolli-Galletti, A. M. submitted to *Macromolecules*
13 Brandup, J. and Immergut, E. H. 'Polymer Handbook', Interscience Publication, New York, 1975
14 Martuscelli, E. *Polym. Eng. Sci.* to be published
Martuscelli, E., Silvestre, C. and Bianchi, L. *Polymer* 1983, **24**, 1458
15 Mandelkern, L. 'Crystallization in Polymers', McGraw-Hill, New York, USA, 1964
16 Hoffman, J. D. *SPE Trans.* 1964, **4**, 315
17 Hoffman, J. D., Davis, G. T. and Lauritzen, J. I. in 'Treatise on Solid State Chemistry' (Ed. ?. ?. Hannay), Plenum Press, New York, 1976, Vol. 3, Ch. 7
18 Williams, H. L., Landel, R. F. and Ferry, J. D. *J. Am. Chem. Soc.* 1955, **77**, 3701
19 Crispino, L., Martuscelli, E. and Pracella, M. *Makromol. Chem.* 1980, **181**, 1747